

Room temperature molten salt as electrolyte for carbon nanotube-based electric double layer capacitors

Bin Xu^{a,b}, Feng Wu^{a,*}, Renjie Chen^a, Gaoping Cao^b,
Shi Chen^a, Guoqing Wang^a, Yusheng Yang^b

^a School of Chemical Engineering and Environment, Beijing Institute of Technology, Beijing 100081, China

^b Research Institute of Chemical Defense, Beijing 100083, China

Received 15 July 2005; received in revised form 28 August 2005; accepted 30 August 2005

Available online 17 November 2005

Abstract

Electric double layer capacitors (EDLCs) have been assembled with carbon nanotubes (CNTs) as the electrodes and a novel binary room temperature molten salt (RTMS) composed of lithium bis(trifluoromethane sulfone)imide ($\text{LiN}(\text{SO}_2\text{CF}_3)_2$, LiTFSI) and acetamide as the electrolyte. The electrochemical performances of the RTMS and the EDLC are evaluated with cyclic voltammetry (CV), ac impedance spectroscopy and galvanostatic charge/discharge, etc. The EDLC with these components show excellent electrochemical properties in specific capacitance, rate and cycling performances at ambient and elevated (60 °C) temperatures, indicating that RTMS is a promising electrolyte for advanced EDLCs.

© 2005 Elsevier B.V. All rights reserved.

Keywords: Room temperature molten salt; Electrolyte; Electric double layer capacitor; Capacitance; Carbon nanotube electrode

1. Introduction

Electric double layer capacitors (EDLCs) have attracted great attention in recent years because of their wide potential applications in electric vehicles and other high-power apparatuses due to their high-power density and long cycling life [1–3]. Since the electric energy stored in EDLCs are given rise by the separation of charged species in the electric double layer across the electrode/electrolyte interface, the performance of the EDLCs depend strongly on the electrolyte and the specific surface area of the electrode materials. Both aqueous and non-aqueous organic solutions can be used as electrolytes for EDLCs. However, EDLCs with non-aqueous electrolytes can work in a wider range of voltage and therefore, can store more energy than those with aqueous electrolytes. It is well-known that traditional non-aqueous electrolyte tends to absorb moisture from the environment, resulting in performance deterioration. In addition, the application of volatile and flammable organic solvent makes the EDLCs unable and even results in safety concerns at high temperatures.

Room temperature molten salt (RTMS) is also known as ionic liquid (IL) because it is liquid at ambient or even lower temperatures and composed entirely of ions. They are regarded as potential safer electrolytes due to their unique physical and chemical properties such as wide temperature range as a liquid, high thermal stability, negligible vapor pressure, non-toxicity, rather high ionic conductivity, high electrochemical stability, etc. RTMS has been applied in a variety of electrochemical devices including lithium rechargeable batteries [4–6], EDLCs [7–13] and solar cells [14]. Compared with conventional organic electrolyte, RTMS electrolyte can improve the safety and capacity retention of the EDLCs at high temperatures.

Studies of RTMS electrolytes for EDLCs at present are focused on those composed of imidazolium-type cations (such as 1-ethyl-3-methylimidazolium (EMI)) and various anions [7–10], due to their low viscosity and high ionic conductivity. However, the low cathodic stability hinders their practical applications. Recently, Sato and co-workers [12,13] synthesized ionic liquids containing *N,N*-diethyl-*N*-methyl-*N*-(2-methoxyethyl)ammonium (DEME) cation and BF_4 or TFSI anion and applied them in EDLCs. Although their EDLCs had a higher capacity and a better charge/discharge cycling durability than those with non-aqueous electrolyte (1 M TEA- BF_4 /PC, for example) at high temperature, a fatal drawback was the

* Corresponding author. Tel.: +86 10 68912508; fax: +86 10 68451429.
E-mail address: wufeng863@vip.sina.com (F. Wu).

high viscosity of this RTMS, hindering its practical application when high-power EDLCs are required. In addition, as most of the few reports involving the application of RTMS in EDLCs are focused on the performance of the electrolyte itself, data on the performance of the EDLCs are a scarcity. Previously, we reported a series of novel and cheap RTMSs based on lithium bis(trifluoromethane sulfone)imide (LiN(SO₂CF₃)₂, LiTFSI) and organic compounds with acylamino group [15–20]. Among them, the RTMSs composed of LiTFSI and acetamide are believed promising electrolytes for electrochemical devices due to their excellent thermal stability, low viscosity at room temperature [18], high ionic conductivity and broad electrochemical stability as shown in the following.

It is well-known that only the surface of the pores that the ions can access can contribute to the double layer capacitance of the EDLCs. Activated carbons with very high specific surface area (>1000 m² g⁻¹) are often used as electrode materials for EDLCs [21]. However, a significant portion of their surface area cannot contribute to the double layer capacitance even in aqueous electrolytes because the inaccessible micropores contribute the most to the total surface area of the material. The bigger the solvated ions are, the larger the pore size of the carbon materials is required. Therefore, the ratio of the usable surface area to the total surface area of the activated carbons is very low when organic electrolytes with large solvated ions are used. In addition, the poor electric conductivity of the activated carbon materials and low mobility of the ions in the micropores strongly affect the power density of EDLCs. In contrast, the well-developed mesopores of carbon nanotubes (CNTs) are highly accessible for both small ions in aqueous electrolyte and large ions in organic electrolyte. As the size of the ions in our RTMS is much larger than those in conventional aqueous electrolyte, CNTs is a better choice than the activated carbon as the electrode material. Therefore, combined with its high electric conductivity, chemical stability and other beneficial features, CNTs is of great interest as an electrode material for EDLCs [22–24].

In this paper, we will evaluate the electrochemical performances of a specific recipe of these RTMSs as electrolyte in EDLC with carbon nanotube electrode by cyclic voltammetry, galvanostatic charge/discharge and ac impedance spectroscopy, etc. Our finding indicates that LiTFSI-acetamide molten salt shows excellent electrochemical performances as electrolyte for the EDLCs.

2. Experimental

2.1. Carbon nanotubes

The CNTs were obtained by catalytic pyrolyzing of C₂H₂/H₂ with powder Ni as the catalyst. Later nitric acid was employed to remove the residual powder from the CNTs. The resultant CNTs were 10–30 nm in diameter. Specific surface area and pore structure were determined with N₂ adsorption/desorption isotherms at 77 K (Quantachrome NOVA 1200). The main parameters of the microtexture of the CNTs are shown in Table 1.

Table 1
Porous texture of the carbon nanotubes

	CNTs
S_{BET} (m ² g ⁻¹)	193
V_{tot} (cm ³ g ⁻¹)	0.449
V_{mic} (cm ³ g ⁻¹)	0.022
V_{mes} (cm ³ g ⁻¹)	0.427
$V_{\text{mes}}/V_{\text{tot}}$ (%)	95.1
D (nm)	9.31

S_{BET} : BET specific surface area; V_{tot} : total pore volume; V_{mic} : micropore volume; V_{mes} : mesopore volume; D : average pore diameter.

2.2. RTMS electrolyte

LiTFSI (3M Inc., 99%) and acetamide (Acros Inc., AP) were dried under vacuum at 140 °C for 12 h and 55 °C for 10 h, respectively. The RTMS electrolyte was prepared by simply mixing LiTFSI and acetamide with a molar ratio of 1:6.0 in an argon-filled MBraun LabMaster 130 glovebox (H₂O < 5 ppm).

The melting points of the RTMS electrolytes were determined with a DSC 2010 differential scanning calorimeter (TA Inc.). Ionic conductivity measurements were carried out in an electrochemical cell with Pt electrode. Its cell constant was determined with a standard KCl solution (0.01 mol L⁻¹) at 25 °C. The ac impedance of the sample was measured with a CHI660A electrochemical workstation (1 Hz–100 KHz, 0–80 °C). The electrochemical window of the molten salt was measured with cyclic voltammogram (CV) on the electrochemical workstation at a scan rate of 0.1 mV s⁻¹ at 25 °C. The sample was sealed in a glass cell with platinum wire (ϕ = 0.1 mm) as the working electrode and Li foil (99.9%) as the reference and counter electrodes. All the cells were assembled in the glovebox.

2.3. Fabrication of EDLC

A mixture of 87 wt.% CNT, 10 wt.% acetylene black and 3 wt.% PTFE binder were pressed into pellets (11 mm in diameter) as electrodes. Then the electrodes were dried under vacuum at 120 °C for 12 h. Button-type capacitor was assembled with two CNT electrodes separated with a polypropylene membrane, all soaked in the as-prepared molten salt electrolyte, in an Ar-filled glovebox (MBraun LabMaster 130).

2.4. Evaluation of EDLC performance

The cyclic voltammetry (CV) and impedance spectra were recorded on an electrochemical workstation IM6e (Germany). The frequency range for the impedance spectra was from 0.01 Hz to 1 MHz. Equivalent series resistance (ESR) was measured at 1 kHz. The galvanostatic charge/discharge (I = 0.28 mA, \sim 0.3 mA cm⁻²) was carried out on a Land cell tester. The specific capacitance (C) of a single CNT electrode was determined with the formula $C = 2It/\Delta Vm$, where I is the discharge current, t is the discharge time, ΔV is the potential change in discharge and m is the mass of the active electrode material. The capacitors were cycled between 0 and 2 V unless specified.

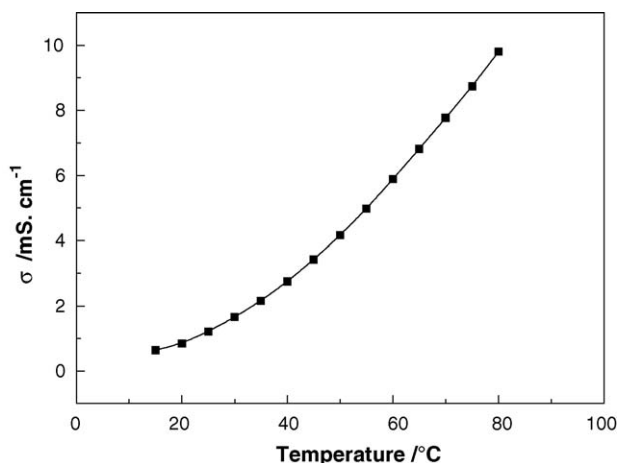


Fig. 1. The temperature-dependent ionic conductivity of the RTMS at LiTFSI:acetamide = 1:6.0.

3. Results and discussion

3.1. Characterization of LiTFSI-acetamide molten salt

DSC analysis shows that the LiTFSI-acetamide molten salt has the excellent thermal stability and its eutectic temperature is $-59\text{ }^{\circ}\text{C}$, lower than the melting points of LiTFSI ($234\text{ }^{\circ}\text{C}$) and acetamide ($81\text{ }^{\circ}\text{C}$). Spectroscopic and theoretical studies [17,20] indicate that acetamide works as complexing agent for both the cations and anions due to its two polar groups (C=O and NH_2 group), weakening and even breaking the bonding between the Li^+ cations and TFSI $^-$ anions. This interaction results in the formation of RTMS.

The temperature-dependent ionic conductivity of the LiTFSI-acetamide molten salt is shown in Fig. 1. The conductivity increases gradually as the temperature rises from 15 to $80\text{ }^{\circ}\text{C}$. It reaches $1.21 \times 10^{-3}\text{ S cm}^{-1}$ at $25\text{ }^{\circ}\text{C}$ and rises to $5.89 \times 10^{-3}\text{ S cm}^{-1}$ at $60\text{ }^{\circ}\text{C}$. The Arrhenius plot (inset of Fig. 2.) is a curved profile, indicating that the conductivity–temperature dependence does not obey the Arrhenius equation. However, this relation fits well to the VTF equation (Fig. 2), implying a solvent-assisted ionic conduction mechanism.

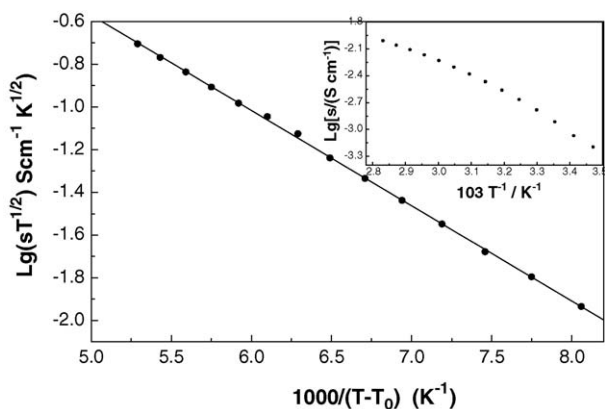


Fig. 2. The VTF plot of the conductivity for the RTMS electrolyte (inset: Arrhenius plots of the conductivity for the RTMS electrolyte).

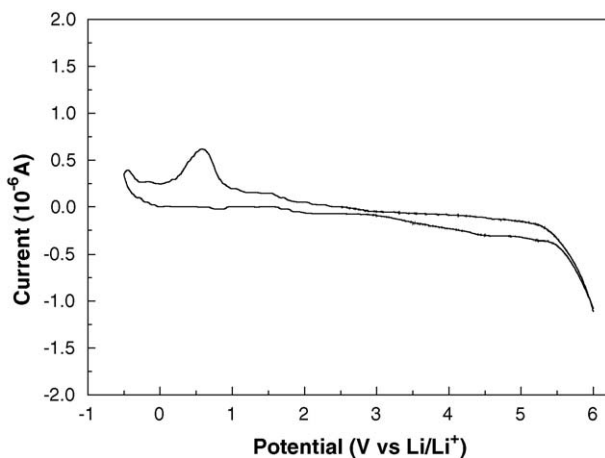


Fig. 3. Cyclic voltammogram for RTMS with platinum wire ($\phi=0.1\text{ mm}$) as the working electrode and Li foil as the reference and counter electrodes (scan rate = 50 mV s^{-1} ; $T=25\text{ }^{\circ}\text{C}$).

anism. This may be attributed to the strong interaction between LiTFSI and acetamide [20].

A micro-electrode cell with platinum wire ($\phi=0.1\text{ mm}$) as the working electrode and Li foil (99.9%) as the reference and counter electrodes was assembled to determine the electrochemical stability window of the LiTFSI/acetamide electrolyte by cyclic voltammetry at $25\text{ }^{\circ}\text{C}$ (Fig. 3). A reduction peak and an oxidation peak are observed at 0.6 and 5.3 V, respectively. Therefore, the electrochemical stability window of the molten salt on Pt is about 4.7 V.

3.2. Evaluation of molten salt as electrolyte for EDLCs

Fig. 4 shows the cyclic voltammogram of the capacitor with RTMS as electrolyte between 0 and 1.0 V at 5 mV s^{-1} scan rate. The well-defined rectangular voltammogram indicates a pure electrostatic attraction, i.e. a typical capacitive behavior. The CV curves of the EDLC in different potential ranges are shown in Fig. 5. The curves in all the tested potential ranges are like

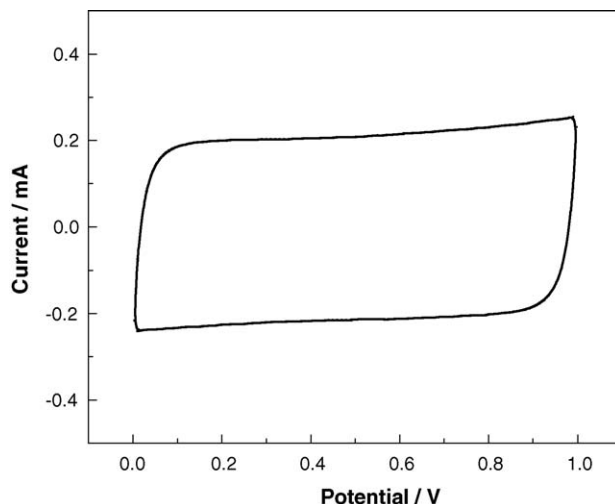


Fig. 4. Cyclic voltammogram of an EDLC built from CNTs in RTMS electrolyte, scan rate: 5 mV s^{-1} .

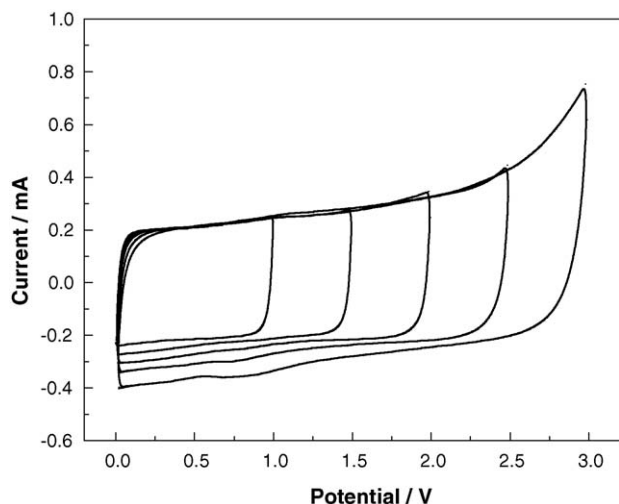


Fig. 5. Cyclic voltammetry at different potential range of an EDLC built from CNTs in RTMS electrolyte, scan rate: 5 mV s^{-1} .

boxes, characteristic of EDLC. An oxidation peak was observed when the cutoff charge voltage increases to 3.0 V. Therefore, the operation voltage of the EDLC can reach 2.5 V, rather high for capacitors but much lower than the above determined electrochemical stability window of the RTMS. Similar observations have been reported previously [9]. An explanation is that the electrodes of the actual capacitor are composed of porous carbons with various active functional groups on their surfaces, while the stability window of the RTMS is usually determined on inert electrodes such as glassy carbon and platinum.

Galvanostatic charge/discharge (0.3 mA cm^{-2}) is performed to determine the capacitance of the active materials. In order to ensure the stable electrochemical performances, the voltage range of charge/discharge is limited between 2.0 and 0.0 V. The linear voltage–time dependence demonstrates the typical capacitive behavior of the cell (Fig. 6). The efficiency of the capacitor is estimated as $\Delta t_d/\Delta t_c \times 100\%$, where Δt_d and Δt_c represents the discharge and charge time, respectively. The coulomb-

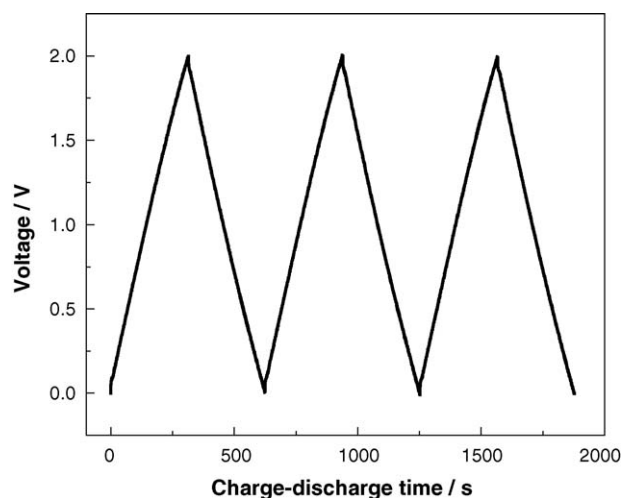


Fig. 6. Charge–discharge curves of an EDLC built from CNTs in RTMS electrolyte.

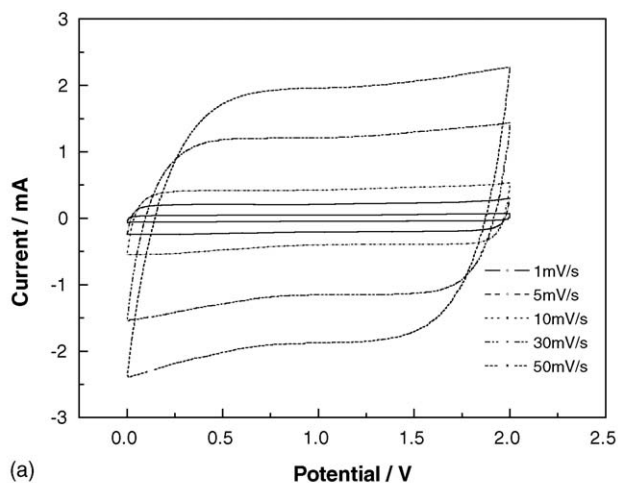
bic efficiency reaches 98.4%, implying good charge/discharge reversibility for the capacitor. The specific capacitance of the cell is determined to be 22 F g^{-1} , very close to the same capacitor with 6 mol L^{-1} KOH aqueous electrolyte (25 F g^{-1}). The capacitance of the EDLC can also be estimated with CV curves using equation $c = i/v$, where i and v are the current and the potential scan rate, respectively. The specific capacitance at scan rate 1 mV s^{-1} is 22 F g^{-1} , consistent with that obtained from galvanostatic cycling at 0.3 mA cm^{-2} .

In the EDLCs, the stored energy is based on the separation of charges across the electrode/electrolyte interface. The electrode surface must be electrochemically accessible for the ions. Therefore, the better developed are the pores of the electrode material, the higher will be the rate of charge accumulation and release. Clearly, the size of the solvated anions and cations are much larger in organic electrolyte than in aqueous electrolyte. As a result, the capacitance of some microporous carbon in non-aqueous electrolyte is much lower than in aqueous electrolyte. Table 1 indicates that the CNT electrode material has a developed mesoporous structure. Consequently, the surface area of the CNT is highly accessible not only for the ions in aqueous electrolyte but also for the larger ions in the molten salt. As a result, the capacitance of the cell with RTMS is very close to that with aqueous electrolyte. However, the energy density of the EDLC with RTMS electrolyte is much higher than that with aqueous electrolyte because the former can be operated at a higher voltage ($W = CV^2/2$).

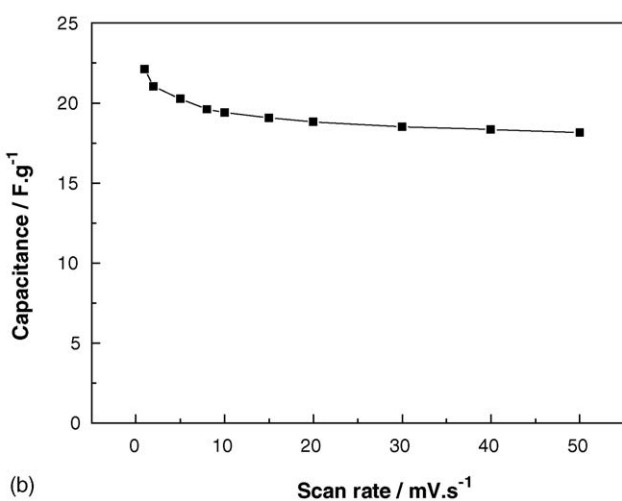
Rate capability is an important feature of the EDLCs. The rectangular cyclic voltammograms of the EDLC over a wide range of scan rates (Fig. 7a) reflect the ability of the RTMS-based EDLCs to cycle at high current densities. Until the scan rate increases to 50 mV s^{-1} , the voltammetric curve still remains rectangular. Fig. 7b shows the influence of potential scan rate on the capacitance recorded at scan rates from 1 to 50 mV s^{-1} . The specific capacitance decreases gradually as the potential scan rate increases. As the scan rate rises to 50 mV s^{-1} , the specific capacitance decreases to 18 F g^{-1} , 82% of that measured at a scan rate of 1 mV s^{-1} . The slight capacitance decay at higher potential scan rates implies the good rate performance of the capacitor due to the high ionic conductivity of the RTMS and the highly mesoporous structure of the CNTs.

Fig. 8 shows the cycling performance of the EDLC between 0 and 2.0 V at room temperature ($I = 0.28 \text{ mA}$). A high capacitance retention is obtained over prolonged cycling test. The capacity decay was about 10% of the initial discharge capacity after 1000 cycles.

The most attractive characteristics of the RTMS electrolytes are their outstanding thermal performances such as high thermal stability, non-flammability and low vapor pressure. The galvanostatic charge/discharge voltage profiles at 20, 40 and 60°C at the same current density (Fig. 9) all retain an isosceles triangle shape, indicating typical capacitive behavior. The specific capacitance increases from 22 F g^{-1} at 20°C to 26 F g^{-1} at 40°C and 30 F g^{-1} at 60°C . It is well-known that the resistance of the electrolyte, sensitive to temperature, strongly affects the capacitor performance. Therefore, the increasing capacitance with the increasing temperature is mainly attributed to



(a)



(b)

Fig. 7. (a) Cyclic voltammetry of CNTs in RTMS electrolyte at different scan rate; (b) specific capacitance based on CNTs as a function of scan rate.

the decreasing resistance of the RTMS electrolyte (Fig. 1). Usually, the coulombic efficiency will drop at high temperature due to the decomposition of the electrolyte. However, the coulombic efficiency of our EDLCs with the novel RTMS electrolyte only

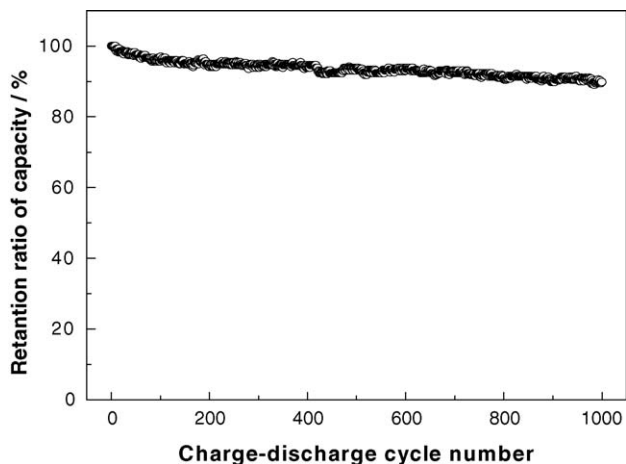


Fig. 8. Cycle test of an EDLC using RTMS as an electrolyte.

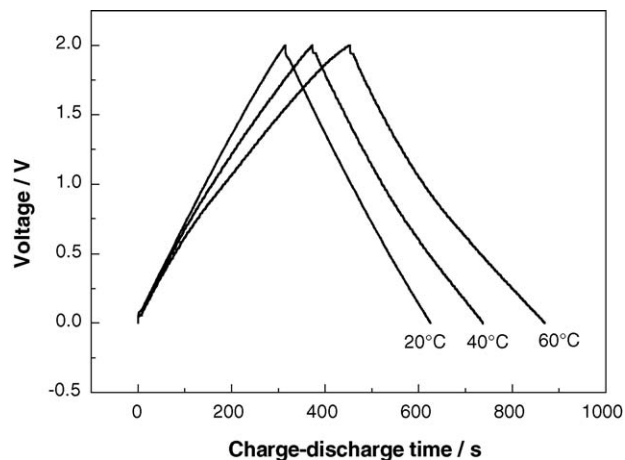


Fig. 9. Charge-discharge curves of an EDLC using RTMS electrolyte at 20, 40, and 60 °C.

drops slightly from 98.4% at 20 °C to 97.6% at 40 °C, and then to 91.8% at 60 °C, much higher than the EDLCs with EMI-BF₄ or DEME-BF₄ molten salt electrolyte [12]. This indicates that the EDLCs with LiTFSI/acetamide molten salt are more stable than those with other RTMSs at high temperature.

The effect of temperature on the performance of the capacitor is further investigated with electrochemical impedance spectroscopy. The impedance behavior of the CNT electrode in the RTMS electrolyte was similar to that previously observed in both aqueous and non-aqueous electrolytes [25–27]. The shape of the Nyquist plots of the electrolyte are similar to each other at different temperatures (Fig. 10), composed of a semicircle at high frequency and an nearly vertical line at low frequency, where

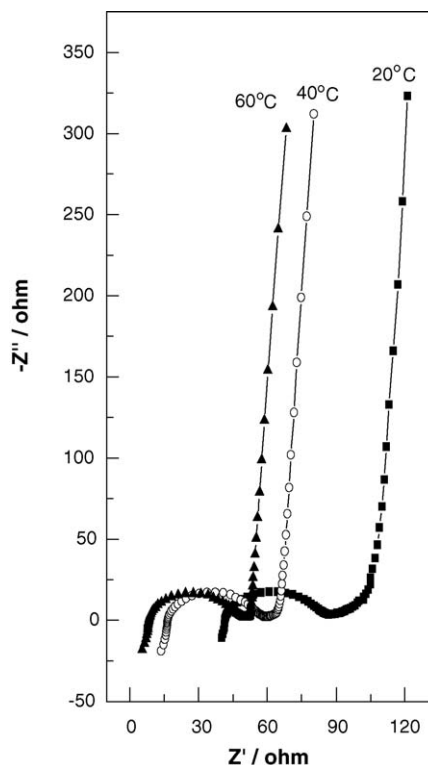


Fig. 10. Nyquist plots of an EDLC using RTMS electrolyte at 20, 40, and 60 °C.

the behavior becomes mainly capacitive. The Nyquist plots at 20 °C still has a sloping (ca. 45°) linear region at high-to-medium frequency, indicating that diffusion control is the limiting factor in the kinetic of the electrode process because of the large diffusion resistance [28]. The slope increases and the length of the 45° region decreases in the Nyquist plot as the temperature increases to 40 °C. When the temperature increases to 60 °C, the sloping linear region becomes hardly recognizable. The equivalent series resistance is also a function of the temperature. It decreases from 77.8 Ω at 20 °C to 40.5 Ω at 60 °C. The decrease of diffusion resistance and ESR with increasing temperature, beneficial for obtaining high-power density, can be attributed to the increasing ionic conductivity and decreasing viscosity of the RTMS electrolyte. As the temperature increases, the specific capacitance of the EDLC increases while the equivalent series resistance decreases. Hence, a higher energy density and power density can be obtained at higher temperatures. On the contrary, the performances of EDLCs with conventional organic electrolyte would have been severely deteriorated and might result in safety concerns at so high temperatures due to the application of volatile and flammable organic solvent. Obviously, the LiTFSI-acetamide molten salt is superior to the conventional aqueous or organic electrolytes, especially at high temperatures.

4. Conclusions

Room temperature molten salt LiTFSI-acetamide has been synthesized and used as electrolyte for electric double layer capacitors. This electrolyte shows excellent thermal stability, high ionic conductivity and wide electrochemical stability window on carbon nanotubes electrode. As a result, the EDLC with RTMS electrolyte can be charged up to 2.5 V with good rate performance and high capacitance retention. The specific capacitance based on carbon nanotubes reaches 22 F g⁻¹ at 20 °C. As the temperature increases to 60 °C, the specific capacitance of the EDLC increases to 30 F g⁻¹ while its equivalent series resistance decreases to 40.5 Ω. Therefore, higher energy density and power density can be expected at high temperatures for this capacitor. Coupled to its excellent thermal stability and safety, this RTMS has prominent advantages as electrolyte for EDLCs with high energy density.

Acknowledgement

This work was financially supported by National Key Basic Research and Development Program (973 Program, 2002CB211800) and the National Key Program for Basic Research of China (2001CCA05000). The authors thank Z.X. Wang (Laboratory for Solid State Ionics, Institute of Physics,

Chinese Academy of Sciences) and C.M. Hong (College of Chemistry and Molecular Engineering, Peking University) for a critical reading of this manuscript.

References

- [1] L.P. Jarvis, T.B. Atwater, P.J. Cygan, *J. Power Sources* 79 (1999) 60–63.
- [2] R.A. Huggins, *Solid State Ionics* 134 (2000) 179–195.
- [3] A. Chu, P. Braatz, *J. Power Sources* 112 (2002) 236–246.
- [4] H. Sakaebe, H. Matsumoto, *Electrochim. Commun.* 5 (2003) 594–598.
- [5] B. Garcia, S. Lavallée, G. Perron, C. Michot, M. Armand, *Electrochim. Acta* 49 (2004) 4583–4588.
- [6] T. Sato, T. Maruo, S. Marukane, K. Takagi, *J. Power Sources* 138 (2004) 253–261.
- [7] M. Ue, M. Takeda, T. Takahashi, M. Takehara, *Electrochim. Solid-State Lett.* 5 (2002) A119–A121.
- [8] A. Balducci, U. Bardi, S. Caporali, M. Mastragostino, F. Soavi, *Electrochim. Commun.* 6 (2004) 566–570.
- [9] A. Lewandowski, M. Galinski, *J. Phys. Chem. Solids* 65 (2004) 281–286.
- [10] M. Ue, M. Takeda, A. Toriumi, A. Kominato, R. Hagiwara, Y. Ito, *J. Electrochem. Soc.* 150 (2003) A499–A502.
- [11] J.N. Barisci, G.G. Wallace, D.R. MacFarlane, R.H. Baughman, *Electrochim. Commun.* 6 (2004) 22–27.
- [12] T. Sato, G. Masuda, K. Takagi, *Electrochim. Acta* 49 (2004) 3603–3611.
- [13] Y.J. Kim, Y. Matsuzawa, S. Ozaki, K.C. Park, C. Kim, M. Endo, H. Yoshida, G. Masuda, T. Sato, M.S. Dresselhaus, *J. Electrochem. Soc.* 152 (2005) A710–A715.
- [14] N. Papageorgiou, Y. Athanassov, M. Armand, P. Boñhote, H. Pettersson, A. Azam, M. Grätzel, *J. Electrochem. Soc.* 143 (1996) 3099–3108.
- [15] H.Y. Liang, H. Li, Z.X. Wang, F. Wu, L.Q. Chen, X.J. Huang, *J. Phys. Chem. B* 105 (2001) 9966–9969.
- [16] H.Y. Liang, F. Wu, L.Q. Chen, X.J. Huang, *Chem. J. Chin. Univ.* 24 (2003) 305–309.
- [17] R.J. Chen, F. Wu, H.Y. Liang, C.Z. Zhang, *Chem. J. Chin. Univ.* 25 (2004) 2108–2111.
- [18] Y.S. Hu, H. Li, X.J. Huang, L.Q. Chen, *Electrochim. Commun.* 6 (2004) 28–32.
- [19] R.J. Chen, F. Wu, H.Y. Liang, L. Li, B. Xu, *J. Electrochem. Soc.* 152 (2005) A1979–A1984.
- [20] R.J. Chen, F. Wu, L. Li, H.Y. Liang, *J. Phys. Chem. B*, submitted for publication.
- [21] E. FracPPkowiak, F. Béguin, *Carbon* 39 (2001) 937–950.
- [22] C. Niu, E.K. Sichel, R. Hoch, D. Moy, H. Tennent, *Appl. Phys. Lett.* 70 (1997) 1480–1482.
- [23] K.H. An, W.S. Kim, Y.S. Park, Y.C. Choi, S.M. Lee, D.C. Chung, D.J. Bae, S.C. Lim, Y.H. Lee, *Adv. Mater.* 13 (2001) 497–500.
- [24] F. Pico, J.M. Rojo, M.L. Sanjuan, A. Anson, A.M. Benito, M.A. Callejas, W.K. Maser, M.T. Martinez, *J. Electrochem. Soc.* 151 (2004) A831–A837.
- [25] E. Frackowiaka, K. Metenier, V. Bertagna, F. Begiun, *Appl. Phys. Lett.* 77 (2000) 2421–2423.
- [26] E. Lust, G. Nurk, A. Janes, M.A.P. Nigu, P. Möller, S.K.V. Sammelselg, *J. Solid State Electrochem.* 7 (2003) 91–105.
- [27] M. Toupina, D. Bélanger, I.R. Hillb, D. Quinnc, *J. Power Sources* 140 (2005) 203–210.
- [28] K. Okajima, K. Ohta, M. Sudoh, *Electrochim. Acta* 50 (2005) 2227–2231.